

Some prospects for ensemble solid-state NMR quantum computers

A. A. Kokin, K. A. Valiev

Institute of Physics and Technology of RAS, 34, Nakhimovskii pr., 117218 Moscow, Russia

Abstract

As an ensemble scheme of solid-state NMR quantum computers the extension of Kane's many-qubits silicon scheme based on the array of ^{31}P donor atoms are spaced lengthwise of the strip gates is considered. The possible planar topology of such ensemble quantum computer is suggested. The estimation of the output NMR signal was performed and it was shown that for the number $N \geq 10^5$ of ensemble elements involving $L \sim 10^3$ qubits each, the standard NMR methods are usable.

As main mechanisms of decoherence for low temperature ($< 0.1\text{K}$), the adiabatic processes of random modulation of qubit resonance frequency determined by secular part of nuclear spin hyperfine interaction with electron magnetic moment of basic atom and dipole-dipole interaction with nuclear moments of neighboring impurity atoms was considered, It was made estimations of allowed concentrations of magnetic impurities and of spin temperature whereby the required decoherence suppression is obtained. Semiclassical decoherence model of two qubit entangled states is also presented.

As another variant of the solid-state ensemble quantum computer, the gateless architecture of cellular-automaton with antiferromagnetically ordered electron spins is also discussed here.

Introduction

Atomic nuclei with spin quantum number $I = 1/2$ are the *natural candidates* for qubits in quantum computers. The early approach to NMR quantum computers was suggested in 1997 [1, 2] and then confirmed in experiments [3, 4]. In this approach several diamagnetic organic liquids whose individual molecules, having a number of interacted non-equivalent nuclear spins-qubits with $I = 1/2$ and being nearly independent on one another where used. They act in parallel as an ensemble of *almost independent* quantum molecules-microcomputers. In so doing the nuclear spins of an individual molecule are described by mixed state density matrix of *reduced quantum ensemble*. *Initialization* of the nuclear spin states in this case means the transformation of mixed state into so called, effective or *pseudo-pure* state [1, 2, 4, 5].

The access to individual qubits in a liquid sample is replaced by simultaneous access to related qubits in all molecules of a bulk ensemble. Computers of this type are called *bulk-ensemble* quantum computers. The liquid-based quantum computer can operate at *room temperature*. For control and measurements of qubit states the standard NMR technique is used.

The principle one-coil scheme of experiment is shown in Fig. 1. The sample is placed in the constant external magnetic field \mathbf{B} and in the alternating (say, linearly polarized) field $\mathbf{b}(t)$, produced by RF voltage $V_\omega(t)$:

$$\mathbf{B}(t) = \mathbf{B} + \mathbf{b}(t) = B\mathbf{k} + 2b \cos(\omega t + \varphi)\mathbf{i}, \quad (1)$$

where \mathbf{i} and \mathbf{k} are unit vectors along the axes x and z.

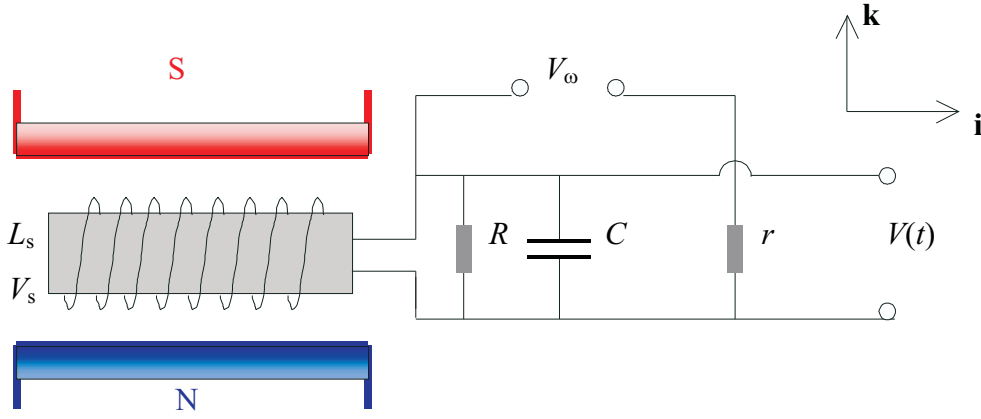


Fig. 1. The principle one-coil scheme of NMR measurement.

Let the sample represent an ensemble of N molecules–microcomputers with L qubits each at temperature $T = 300$ K, in the external magnetic fields $B = 1 - 10$ T. The resonance nuclear spin frequency is $\omega_A/2\pi \sim \gamma_I B/2\pi < 150$ MHz, γ_I is gyromagnetic ratio of nuclear spin ($\gamma_I \sim \gamma_N = 95.8$ radMHz/T), $\hbar\omega_A/kT < 10^{-5}$.

The output oscillating voltage $V(t)$ is

$$V(t) = QKd\Phi(t)/dt = \mu_0 QKAdM_x(t)/dt, \quad (2)$$

where $\Phi(t) = \int_A \mu_0 M_x(t) dydz$ is magnetic flux produced by resonant spins in the coil ($\mu_0 = 4\pi \cdot 10^{-1} \text{T}^2 \text{cm}^3/\text{J}$), $L_s = \mu_0(KA)^2/V_s$ is solenoid inductance of the resonance counter, V_s is volume of the solenoid, K is the number and A is area of coil turns, $Q = R/(\omega_A L_s) > 10^2$ is the *quality factor* of resonance counter for parallel connected resistance R (Fig. 1). For resonance condition $\omega = \omega_A = (L_s C)^{-1/2}$.

The maximum nuclear spin read-out magnetization $M_{x\text{max}}$ (the liquid sample is considered here to be a continuous medium and to have volume $V \sim V_s$) at *optimum resonance condition* is defined by the amplitude of RF field $b = 1/(\gamma_I \sqrt{T_{\perp I} T_{\parallel I}})$ [6] (see also (20) below):

$$M_{x\text{max}} = M_{z\text{m}} \sqrt{T_{\perp I}/T_{\parallel I}}/2 \approx \gamma_I \hbar/2 \cdot (N/V_s) \cdot \varepsilon(L)/2, \quad (3)$$

where $M_{z\text{m}}$ is maximum equilibrium nuclear magnetization, $T_{\perp I}$ and $T_{\parallel I}$ are effective transverse and longitudinal relaxation times, N is number of resonant nuclear spins (one in a molecule) in volume V_s . Parameter $\varepsilon(L)$ is the maximum probability of the full nuclear polarization in pseudo-pure state $P_{\parallel} = 1$ [7]. It may be estimated by the difference of equilibrium population between the lowest and the highest energy states. For nearly homonuclear L spin system [7] it is:

$$\varepsilon(L) = \frac{\exp(L\hbar\omega_A/2kT) - \exp(-L\hbar\omega_A/2kT)}{(\exp(\hbar\omega_A/2kT) + \exp(-\hbar\omega_A/2kT))^L} = \frac{2\sinh(L\hbar\omega_A/2kT)}{2^L \cosh^L(\hbar\omega_A/2kT)}. \quad (4)$$

In the high temperature limit $\hbar\omega_A/(kT) \ll 1$ we have $\varepsilon(L) = L2^{-L}\hbar\omega_A/(kT)$, that is, the signal amplitude *exponentially drops* with the number of qubits, but it *does not drop* for $\hbar\omega_A/(kT) \gg 1$ when $\varepsilon(L) = 1$ (the pure ground nuclear spin quantum state).

The maximum NMR signal intensity S is defined by amplitude

$$S = |V_{\text{max}}| = (\mu_0/4)QKA(N/V_s)\gamma_I \hbar\omega_A \varepsilon(L), \quad (5)$$

where the product KA can also be expressed as

$$KA = (L_s V_s / \mu_0)^{1/2} = (R V_s / (\mu_0 Q \omega_A))^{1/2}. \quad (6)$$

For the root-mean square noise voltage in the measurement circuit we write

$$V_N = \sqrt{4kTR\Delta\nu}, \quad (7)$$

where the amplifier bandwidth is as a rule $\Delta\nu \sim 1$ Hz.

So for *signal to noise ratio* we obtain

$$\begin{aligned} (\text{S/N}) &\equiv |V_{\max}|/V_{\text{N}} \cong \frac{1}{8} \sqrt{\frac{\mu_0 \hbar Q \hbar \omega_{\text{A}}}{\Delta\nu V_{\text{s}} kT}} \gamma_{\text{I}} N \varepsilon(L) \sim \\ &\sim 0.2 \sqrt{(Q/V_{\text{s}}) \cdot (\hbar \omega_{\text{A}}/kT) N \varepsilon(L)} \cdot 10^{-9}, \text{ (here } V_{\text{s}} \text{ in cm}^3\text{)}. \end{aligned} \quad (8)$$

For example, for two qubits molecules ($L = 2$), using, $\varepsilon(L) = \hbar \omega_{\text{A}}/(2kT) \sim 10^{-5}$, we can make an estimation

$$(\text{S/N}) \sim (Q/V_{\text{s}})^{1/2} N \cdot 10^{-16}. \quad (9)$$

Thus, to keep the value $(\text{S/N}) > 1$, the number of resonant nuclear spins for two qubit liquid ensemble at room temperature, $V_{\text{s}} \sim 1 \text{ cm}^3$ and $Q \sim 10^3$ is bound to be $N > 10^{16}$.

In the case of *paramagnetic liquids* one would expect that the number of polarized nuclei may be increased with dynamic polarization (say, Overhauser effect). Assuming electron and nuclear gyromagnetic ratio $\gamma_{\text{e}}/\gamma_{\text{I}} \sim 10^3$ we obtain that in the probability $\varepsilon(L)$ for a L -qubits single state the value $\hbar \omega_{\text{A}}/(kT)$ in (8) should be replaced by $10^3 \hbar \omega_{\text{A}}/(kT)$. Therefore, for the same value $\varepsilon(L)$ and number of molecules N , the allowed number of qubits L approximately will be estimated from

$$L 2^{-L} > 10^{-3}, \quad (10)$$

whence it follows that $L < 12$ qubits.

An additional increase of read-out NMR signal may be obtained in paramagnetic liquids using the ENDOR technique. It is generally believed that for the liquid bulk-ensemble quantum computers a *limiting value* is $L < 20 - 30$ [7].

There are five basic criteria for realization of a *large-scale NMR quantum computer*, which can outperform all traditional classical computers [8]:

1. For any physical system, which presents large-scale quantum register, the necessary number of qubits in quantum register must be $L > 10^3$.

One such example of this register is solid-state homonuclear system, in which nuclear spin containing identical atoms are housed at regular intervals in a natural or an artificial solid-state structure.

2. There is a need to provide the conditions for preparation of initial basic quantum register state. For a many-qubit solid-state NMR quantum computer the quantum register state initializing can be obtained by going to *extra-low nuclear spin temperature* (< 1 mK at fields of order of several tesla).
3. The decoherence time of qubit states T_{d} should be at least up to 10^4 times longer than the ‘clock time’, that is value of order of several seconds for NMR quantum computers. *The decoherence suppression is one of the important problems* in realization of a large-scale quantum computers.
4. There is a need to perform during a decoherence time a set of quantum logic operations determined by a logic unitary transformation. This set should contain certain set of the one-qubit and two-qubits operations are shielded from random errors. The electromagnetic pulses that control the quantum operation should be performed with an accuracy of better than 10^{-4} – 10^{-5} .
5. There is a need to provide *accurate and sensitive read-out measurements of the qubit states*. This is another of the important and hard problems.

The design of solid-state NMR quantum computers was proposed by B. Kane in [9, 10]. It was suggested to use a semiconductor MOS structure on a ^{28}Si spinless substrate, in a near-surface layer whose stable phosphorus isotopes ^{31}P , acting as donors, are implanted in the form of a regular chain.

These donors have a nuclear spin $I = 1/2$ and substitute for silicon atoms at the lattice sites, producing shallow impurity states. The number of donors or the qubit number L in such a quasi-one-dimensional *artificial ‘molecule’* may be arbitrary large. It is suggested an *individual* nuclear spin–qubits electrical control and measurement of qubit states through the use of special gate structures. The experimental implementation of Kane’s scheme is undertaken now in Australian Centre for Quantum Computer Technology [11, 12].

However, there are four essential difficulties in implementing this quantum computer:

1. First of all, signal from the spin of an individual atom is very small and *high sensitive single-spin measurements* are required.
2. For initialization of nuclear spin states it is required to use *very low nuclear spin temperature* (\sim mK).
3. It is required to use regular donors and gates arrangement with high precision in *nanometer scale*.
4. It is necessary to suppress the *decoherence* of quantum states defined by *fluctuations* of gate voltage.

As an alternative, we proposed the variant of *an ensemble silicon-based quantum computer* [13, 14]. One would expect that with the ensemble approach, where many independent ‘molecules’ of Kane’s type work simultaneously, the measurements would be greatly simplified. Here we will give some further development of this scheme.

1 The silicon structure with regular system of strip gates

In this case, unlike the structure suggested in [9], gates **A** and **J** form a chain of narrow ($l_A \sim 10$ nm) and long strips along which donor atoms at l_y distant from each other are placed (Fig. 2). Thus, they form a *regular* structure of the planar silicon topology type.

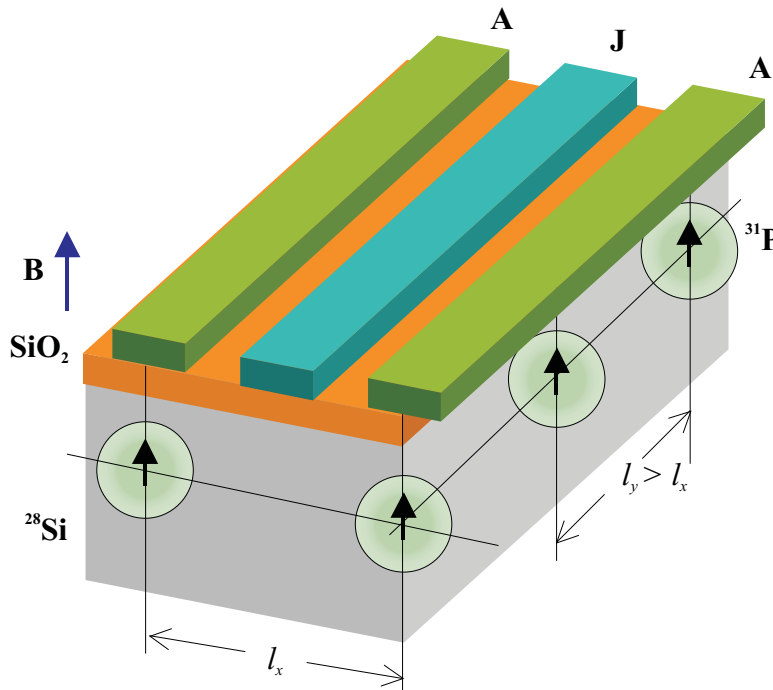


Fig. 2. The structure of two qubit cells for three ensemble component.

The separation between neighboring donor atoms in Si, as in Kane's scheme, must be $l_x \leq 20$ nm. In this case the interqubit interaction is controlled by gates **J**. The depth of donor d is ~ 20 nm. For $l_y \gg l_x$ the exchange spin interaction between electrons of donor atoms disposed along the strip gates (y -axis) is negligibly small. Hence, such a system breaks down into an ensemble of near-independent Kane's artificial 'molecule', whose electronic spins at temperature $T \leq 0.1$ K are initially fully aligned with the field of several Tesla ($\gamma_e \hbar B/kT \gg 1$). As in case of liquids, the nuclear spin states of individual Kane's chain-'molecule' will be described by density matrix of reduced quantum ensemble. Access to individual qubits will be replaced by simultaneous access to related qubits in all 'molecules' of ensemble.

The linear qubit density in the artificial 'molecules' is ~ 50 qubits on micrometer. For the realization of considered structure, as well as of the Kane's scheme, *the nanotechnology* with resolution of the order of ~ 1 nm is also needed.

For *the initializing* of all nuclear spin-qubit quantum states (fully polarized nuclear spins) there is a need to attain, for the time being, nuclear spin temperature $T \leq 10^{-3}$ K. An output signal in this system, as in liquids, will be proportional to the number of 'molecules' or donor atoms N (component number of our ensemble) in the chain along axis y . In the following the lower value of N will be estimated.

2 The states of insulated donor atoms in magnetic fields

The electron-nuclear spin Hamiltonian for a donor atom ^{31}P has the form

$$H = \gamma_e \hbar \mathbf{B} \mathbf{S} - \gamma_I \hbar \mathbf{B} \mathbf{I} + A \mathbf{I} \mathbf{S}, \quad (11)$$

four energy levels of which are given by the well-known Breit-Rabi formula. For $I = 1/2$, $S = 1/2$ (the z -axis is parallel to **B**) this formula is written as

$$E(F, m_F) = -\frac{A}{4} - \gamma_I \hbar B m_F - (-1)^F \text{sign}(1 + m_F X) \frac{A}{2} \sqrt{1 + 2m_F X + X^2}, \quad (12)$$

where constant of hyperfine interaction $A/(2\pi\hbar) = 116$ MHz[15], $X = (\gamma_e + \gamma_I)\hbar B/A \approx \gamma_e \hbar B/A \gg 1$, $F = I \pm 1/2 = 1, 0$, and $m_F = M + m = \pm 1, 0$, if $F = 1$ or $m_F = 0$, if $F = 0$ (Here $M = \pm 1/2$ and $m = \pm 1/2$ are z -projections of electron and nuclear spins accordingly). The energy level scheme is shown in Fig. 3. For the energy of the ground spin state, $F = 0$ and $m_F = 0$, hence, we obtain

$$E(0, 0) = -A/4 - (A/2)\sqrt{1 + X^2}. \quad (13)$$

For the next, excited energy state, $F = 1$, $m_F = -1$ we have

$$E(1, -1) = A/4 - (\gamma_e - \gamma_I)\hbar B/2. \quad (14)$$

Thus, the energy difference between the two lower states of the nuclear spin (the resonant qubit frequency), that interacts with an electron, whose state remains unchanged, is described in simple terms ($\gamma_e \gg \gamma_I$ for $X \approx \gamma_e \hbar B/A \gg 1$):

$$\begin{aligned} \hbar\omega_{\text{A}}^{\dagger} &= E(1, -1) - E(0, 0) = A/2 + (\gamma_I - \gamma_e)\hbar B/2 + \frac{A}{2}\sqrt{1 + X^2} \approx \\ &\approx \gamma_I \hbar B + \frac{A}{2} - \frac{A^2}{4\gamma_e \hbar B}, \\ \hbar\omega_{\text{A}}^{-} &= E(1, 1) - E(1, 0) \approx -\gamma_I \hbar B + \frac{A}{2} + \frac{A^2}{4\gamma_e \hbar B}. \end{aligned} \quad (15)$$

For ^{31}P donor atoms $\gamma_e/\gamma_I = 1.62 \cdot 10^3$, $\gamma_e = 176.08$ radGHz/T, $\gamma_I = 1.13\gamma_N = 108$ radMHz/T. In magnetic field $B = 1$ T: $\omega_{\text{A}}^{\dagger}/2\pi = 75$ MHz, $\omega_{\text{A}}^{-}/2\pi = 41$ MHz.

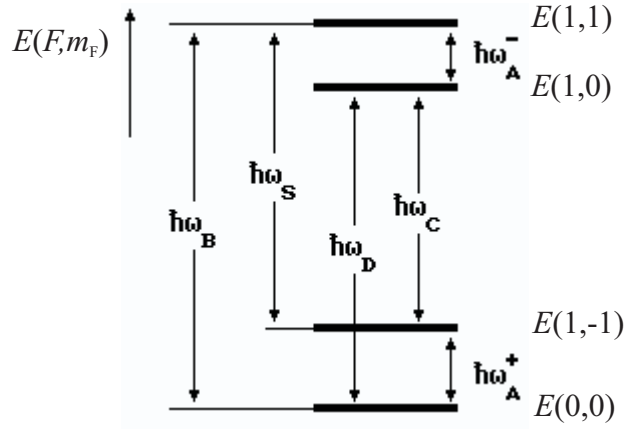


Fig. 3. Energy levels of an individual donor atom in magnetic field.

The frequencies ω_S , ω_B , ω_C , ω_D are in microwave, ω_A^\pm – in the RF ranges of frequencies. The transitions with frequencies ω_S in the first approximation are *forbidden*.

The states $|F, m_F\rangle$ in M, m basis are

$$\begin{aligned}
|1, 1\rangle &= |1/2, 1/2\rangle, \\
|1, -1\rangle &= |-1/2, -1/2\rangle, \\
|1, 0\rangle &= (1 - \alpha)^{1/2} |1/2, -1/2\rangle + \alpha^{1/2} |-1/2, 1/2\rangle, \\
|0, 0\rangle &= (1 - \alpha)^{1/2} |-1/2, 1/2\rangle - \alpha^{1/2} |1/2, -1/2\rangle, \\
\alpha &= \frac{1}{2} \left(1 - \frac{X}{\sqrt{1 + X^2}} \right) \approx 1/(4X^2) \ll 1.
\end{aligned} \tag{16}$$

The diagonal matrix elements of nuclear magnetization M_z per one donor atom for two lower energy states will be determined by

$$\begin{aligned}
\langle 0, 0 | M_z | 0, 0 \rangle &= \langle 0, 0 | I_z | 0, 0 \rangle \gamma_I \hbar = \frac{X}{\sqrt{1 + X^2}} \gamma_I \hbar / 2, \\
\langle 1, -1 | M_z | 1, -1 \rangle &= \langle 1, -1 | I_z | 1, -1 \rangle \gamma_I \hbar = -\gamma_I \hbar / 2.
\end{aligned} \tag{17}$$

The probabilities of the L -qubit lowest and highest energy fully filling states for the same electron spin state $M = -1/2$, which correspond, as noted above, to the maximum probability of the nuclear polarization in pseudo-pure state, are:

$$\begin{aligned}
p^L(1, -1) &= \frac{\exp(-L\hbar\omega_A^+/2kT)}{(\exp(\hbar\omega_A^+/2kT) + \exp(-\hbar\omega_A^+/2kT))^L}, \\
p^L(0, 0) &= \frac{\exp(L\hbar\omega_A^+/2kT)}{(\exp(\hbar\omega_A^+/2kT) + \exp(-\hbar\omega_A^+/2kT))^L}.
\end{aligned} \tag{18}$$

The possible maximum nuclear magnetization M_{zm} (the populations of states $|1, 1\rangle$ and $|1, 0\rangle$ is negligible for $\omega_S, \omega_B, \omega_C \gg \omega_A^\pm$) is

$$\begin{aligned}
M_{zm} &= \gamma_I \hbar / 2 \cdot (N/V_c) \left(\frac{X}{\sqrt{1 + X^2}} \frac{\exp(L\hbar\omega_A^+/2kT)}{(\exp(\hbar\omega_A^+/2kT) + \exp(-\hbar\omega_A^+/2kT))^L} - \right. \\
&\quad \left. - \frac{\exp(-L\hbar\omega_A^+/2kT)}{(\exp(\hbar\omega_A^+/2kT) + \exp(-\hbar\omega_A^+/2kT))^L} \right) = \gamma_I \hbar / 2 \cdot (N/V_c) \varepsilon(L).
\end{aligned} \tag{19}$$

For $L\hbar\omega_A^+/2kT \ll 1$ and $X \gg 1$ we obtain (compare with (3))

$$M_{zm} \approx \gamma_I \hbar / 2 \cdot (N/V_c) \cdot 2^{-L} L (\hbar\omega_A^+/kT). \tag{20}$$

But for very low temperatures ($\hbar\omega_A^+/2kT \gg 1$) we have the *full nuclear polarization* $M_{zm} \approx \gamma_I \hbar / 2 \cdot (N/V_c)$ and $\varepsilon(L) = 1$.

3 The gain effect for NMR signal

Transitions between two lower states are induced by a RF magnetic field, applied at a frequency resonant ω_A^+ . The Rabi resonance frequency Ω , which is defined by matrix elements of spin interaction Hamiltonian with the external RF field $\mathbf{b}(t)$

$$H_{\text{rf}}(t) = (\gamma_e S_x - \gamma_I I_x) \hbar b_x(t), b_x(t) = 2b \cos(\omega_A^+ t) \quad (21)$$

can be found from

$$\Omega = \gamma_I b_{\text{eff}}(X) = 2 |\langle 0, 0 | H_{\text{rf}}(0) | 1, -1 \rangle| / \hbar. \quad (22)$$

For the amplitude of effective RF field, acting on nuclear spin, $b_{\text{eff}}(X)$ we obtain

$$b_{\text{eff}}(X) = b \left(\alpha^{1/2} (\gamma_e / \gamma_I) + (1 - \alpha)^{1/2} \right), \quad (23)$$

where b is the amplitude of circularly polarized field component.

The Rabi frequency has the maximum value for $X = 0$ ($\alpha = 1/2$) and monotonically reduces to value for the insulated nuclear spin ($\alpha \Rightarrow 0$), $\gamma_I b_{\text{eff}}(X \gg 1) = \gamma_I b$. From the rate of quantum operation standpoint it is desirable to operate in relatively weak fields [10], at which $\gamma_e / \gamma_I \gg X \approx \gamma_e \hbar B / A \gg 1$ or $3.5 \text{ T} > B \gg 3.9 \cdot 10^{-3} \text{ T}$.

In this case from (23) we will obtain

$$b_{\text{eff}} = (1 + \eta) b \gg b, \quad (24)$$

where $\eta = A / (2\gamma_I \hbar B) \gg 1$ is the *gain factor*. Under these conditions RF field operates through the transverse component of electronic polarization. For magnetic fields $B = 1 \text{ T}$ we have the value $b_{\text{eff}} = 4.4 \cdot b$, and for $B = 0.01 \text{ T}$ we have the value $b_{\text{eff}} = 338 \cdot b$. The gain effect involves an increase of NMR signal and Rabi frequency. This effect was indicated previously by K. Valiev in [16].

In the pulse technique this effect makes it possible to *decrease the length of pulse* and along with it the times of logic operation performing. Moreover, the computer operations, owing to this effect, can be performed at lower RF fields. At last, it permits to *reduce the RF field influence* on the operation of neighboring semiconductor devices.

To describe the nuclear dynamics for the two low-lying level systems being discussed ($X \gg 1$), we can write the following Bloch-type equation with only two effective relaxation times:

$$\frac{d\mathbf{M}}{dt} = \gamma_I [\mathbf{M} \times \mathbf{B}_{\text{eff}}] - \frac{M_x \mathbf{i} + M_y \mathbf{j}}{T_{\perp I}} - \frac{(M_z - M_{z\text{m}}) \mathbf{k}}{T_{\parallel I}}, \quad (25)$$

where $\mathbf{i}, \mathbf{j}, \mathbf{k}$ are orthogonal unit vectors (Fig. 1), $M_{z\text{m}}$ is defined as (19),

$$\mathbf{B}_{\text{eff}} = (\omega_A / \gamma_I) \mathbf{k} + 2b_{\text{eff}} \cos(\omega t) \mathbf{i}. \quad (26)$$

It follows from it that the value of maximum nuclear read-out magnetization in NMR signal has here for $b_{\text{eff}}(X) = 1 / (\gamma_I \sqrt{T_{\perp I} T_{\parallel I}})$, that is again for $M_{x\text{max}} = M_{z\text{m}} \sqrt{T_{\perp I} / T_{\parallel I}} / 2$. Hence, the read-out *NMR signal can not be increased* through the gain effect over its maximum value, that corresponds to $M_{z\text{m}} \sqrt{T_{\perp I} / T_{\parallel I}} / 2$.

4 The signal to noise ratio for an ensemble silicon quantum computer

For the realization of an ensemble silicon quantum register we propose a variant of planar scheme [17], that, as an example, contains $n \cdot p$ in parallel acting identical blocks, each has N_0 in parallel connected L -qubit Kane's linear 'molecules'. This scheme is schematically depicted in Fig. 4.

Let the sample be the silicon (^{28}Si) plate of thickness 0.1 cm. For the full number of computers-'molecules' in ensemble $N = p \cdot N_0 \cdot n$, the volume of sample and also of solenoid is $V_s \approx \delta \cdot l_x \cdot l_y \cdot L \cdot N$ (the filling factor is assumed for simplicity to be one).

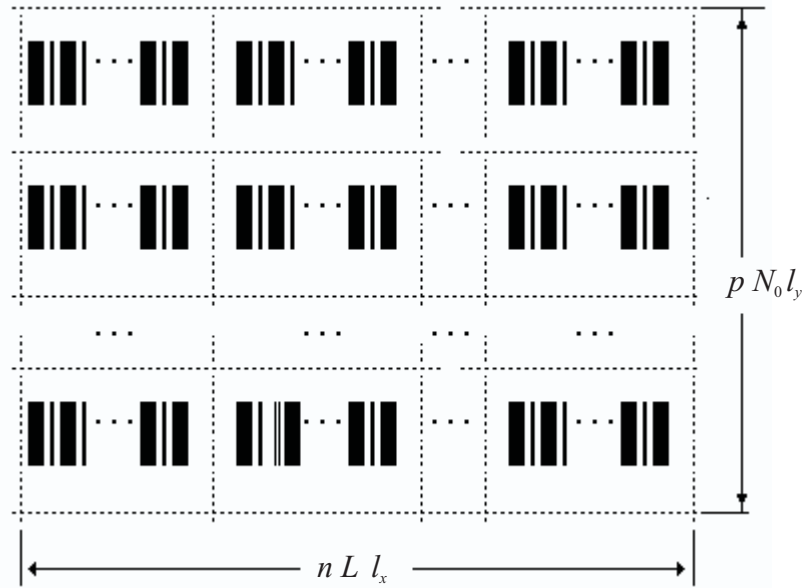


Fig. 4. The scheme of the proposed planar silicon topology with $p \cdot n$ in parallel connected blocks of the ensemble L -qubit quantum computers (the connections are not shown here). The broad and narrow lines denote the **A** and **J** gates.

The read-out signal from such *ensemble in parallel acting* chains, as distinct from liquid prototype, for full nuclear polarization or, what is the same, for nuclear spin temperatures $T_1 \leq 10^{-3}$ K has instead of the small factor in intensity of the NMR signal of type $\varepsilon(L) = 2^{-L} L \cdot \hbar\omega_A / (kT)$ the factor $\varepsilon(L) = 1$. The NMR signal from our sample within a non-essential factor is the same as from macroscopic sample (see Appendix **A.1**). Therefore, with the expressions (4) and (8), $\hbar\omega_A / (kT_1) < 1$ ($T_1 < 1$ mK) and $\varepsilon = 1$ we will obtain as an estimation for maximum signal to noise ratio

$$(S/N) \approx \sqrt{Q\hbar\omega_A / (kTV_s)} \cdot N \cdot 10^{-9} \approx \sqrt{QN / (\delta l_x l_y L)} \cdot 10^{-10}. \quad (27)$$

It is believed that for low temperatures $Q \sim 10^6$. The effective volume of one ‘molecule’ for $l_x = 20$ nm, $l_y = 50$ nm, $L = 10^3$, $V_s = \delta l_x l_y L = 10^{-9}$ cm³ we receive that the read-out signal in our scheme may be *available for standard NMR technique*, if the number of ‘molecules’ in ensemble is of about $N \geq 10^5$. So high-sensitive devices for measurement of individual spin-states are not needed.

To estimate the values n, p let us consider the square plate with $50N_0p = 20 \cdot 10^3 n$ and $N_0 = 100$. As a result, we receive $n \approx 16$ and $p \approx 63$. The area of the structure without passive regions is $\sim 315 \times 315 \mu\text{m}^2$. This size is sufficiently small for sample to be housed in the split between the magnet poles of a standard NMR spectrometer. Real plate may have considerably more area and correspondingly more number of ‘molecules’ N .

For implementation of two-qubit logic operation it is required the controlled by gates **J** interqubit indirect interaction with characteristic frequency $\nu_J \sim 100$ kHz $\ll \omega_A / 2\pi \sim 100$ MHz. To bring about fault-tolerant quantum computations on large-scale quantum computers the relative error for single logic operation must not be more than $\sim 10^{-5}$ [8]. Hence it follows that a *resolution* bound of the NMR spectrometer must be of the order of ~ 100 kHz $\cdot 10^{-5} \sim 1$ Hz, that is consistent with the usual requirements. It is significant that such high precision is needed only for performing the logic quantum operation, but it is not needed for read-out measurements.

The read-out signal may be more increased by means of an electron-nuclear double resonance (ENDOR) methods [18] of observing the electron resonance at transition with frequencies ω_B and ω_C (Fig. 3).

Consequently, by the use of standard NMR and additional of ENDOR techniques *the first main difficulty* of Kane’s scheme can be overcome.

5 The cooling of nuclear spin system and nuclear state initialization by means of dynamic polarization

The electron and nuclear *longitudinal relaxation times* for the *allowed* transitions in four energy level system of phosphorus doped silicon have been extensively investigated experimentally in [18, 19]. For the allowed transitions with frequency ω_B and ω_C (Fig. 3) electron longitudinal relaxation times $\tau_{\parallel B} \approx \tau_{\parallel C}$ at low temperatures were found to be exceedingly long. They are of the order of *one hour* at $T = 1.25$ K, $B \sim 0.3$ T, are independent of phosphorus concentration below $C \sim 10^{16}$ cm $^{-3}$ (mean distance between phosphorus atoms is of the order of 45 nm) and are approximately inversely proportional to the lattice temperature T . The nuclear longitudinal relaxation time T_{\parallel} (the frequency ω_A^+) were found to be equal to 10 hours.

The relaxation time for transition with frequency ω_D , which involves a simultaneous electron-nuclear spin flip-flop, at $T = 1.25$ K, $C \sim 10^{16}$ cm $^{-3}$ and $B \sim 0.3$ T was $\tau_{\parallel D} \sim 30$ hours $\gg \tau_{\parallel B}, \tau_{\parallel C}$.

The *extremely long relaxation times* of the electron and nuclear spins imply that the required initializing of nuclear quantum states (full nuclear *nonequilibrium polarizations*) can be attained by deep cooling of short duration of *only nuclear spin system* to $T_I \leq 1$ mK without deep cooling of the lattice. There is the possibility to reach it at the *indirect cooling* of nuclear spin system by means of *dynamic nuclear spin polarization techniques*[19].

One such method of dynamic nuclear spin polarization for donor atoms is based on the saturation by *the microwave pumping of the forbidden transition* (frequency ω_S in Fig. 3), that is designated as the Abragam's *solid state effect*[6, 19].

Let us consider this effect as applied to the ensemble of ^{31}P atoms. The polarization of electrons $P_S = 2 \langle S_z \rangle$ and of nuclei $P_I = 2 \langle I_z \rangle$ may be for the sake of simplicity expressed as

$$\begin{aligned} P_S &= p(1, 1) + p(1, 0) - p(1, -1) - p(0, 0), \\ P_I &= p(1, 1) + p(0, 0) - p(1, 0) - p(1, -1), \end{aligned} \quad (28)$$

where $p(F, m_F)$ are the populations of states $|F, m_F\rangle$ (Fig. 3). They also fulfill the requirement

$$p(1, 1) + p(1, 0) + p(1, -1) + p(0, 0) = 1. \quad (29)$$

The rate equations for the populations are (it is assumed, that the relaxation rates for transitions at frequencies ω_A^{\pm} are equal to $T_{\parallel A}$):

$$\begin{aligned} dp(0, 0)/dt &= (p(1, 1) - p(0, 0)r_B)/\tau_{\parallel B} + (p(1, 0) - p(0, 0)r_D)/\tau_{\parallel D} + \\ &\quad + (p(1, -1) - p(0, 0)r_A^+)/T_{\parallel A}, \\ dp(1, -1)/dt &= (p(1, 0) - p(1, -1)r_C)/\tau_{\parallel C} + (p(1, 1) - p(1, -1)) \cdot W_e + \\ &\quad + (p(0, 0)r_A^+ - p(1, -1))/T_{\parallel A}, \\ dp(1, 0)/dt &= (p(1, -1)r_C - p(1, 0))/\tau_{\parallel C} + p(0, 0)r_D - p(1, 0)/\tau_{\parallel D} + \\ &\quad + (p(1, 1) - p(1, 0)r_A^-)/T_{\parallel A}, \\ dp(1, 1)/dt &= (p(0, 0)r_B - p(1, 1))/\tau_{\parallel B} + (p(1, -1) - p(1, 1)) \cdot W_e + \\ &\quad + (p(1, 0)r_A^- - p(1, 1))/T_{\parallel A}, \end{aligned} \quad (30)$$

where parameters $r_{B,C,D,A} = \exp(-\hbar\omega_{B,C,D,A}/kT)$ are ratio of rates for an up and down thermal transitions. For values $\hbar\omega_{B,C,D}/kT \gg 1$, $\hbar\omega_A^{\pm}/kT \ll 1$ ($T \leq 0.1$ K) there are the thermal electron $P_{S0} \approx -1$ and nuclear $P_{I0} = \hbar\omega_A^+/kT \ll 1$ polarizations.

Let us assume next that the rate of *induced forbidden electron transitions* $|1, 1\rangle \Rightarrow |1, -1\rangle$ at frequency ω_S , that is W_S and electron longitudinal relaxation times satisfy the conditions:

$$W_S^{-1} < \tau_{\parallel B} \approx \tau_{\parallel C} \ll T_{\parallel A}, \tau_{\parallel D}, \tau_{\parallel S}, \quad (31)$$

where $\tau_{\parallel D}$, $\tau_{\parallel S}$ are the longitudinal relaxation times of electron spins for forbidden transition. Hereafter we shall write

$$\begin{aligned}
dp(0,0)/dt &= p(1,1)/\tau_{\parallel B} + (p(1,-1) - p(0,0))/T_{\parallel A}, \\
dp(1,-1)/dt &= p(1,0)/\tau_{\parallel B} + ((p(1,1) - p(1,-1)) \cdot W_e + (p(0,0) - p(1,-1))/T_{\parallel A}), \\
dp(1,0)/dt &= -p(1,0)/\tau_{\parallel B} + (p(1,1) - p(1,0))/T_{\parallel A}, \\
dp(1,1)/dt &= -p(1,1)/\tau_{\parallel B} + (p(1,-1) - p(1,1)) \cdot W_e + (p(1,0) - p(1,1))/T_{\parallel A}
\end{aligned} \tag{32}$$

With equations (28),(29),(31) we can obtain the rate equations for P_S and P_I :

$$\begin{aligned}
dP_S/dt &= -(P_S + P_I) \cdot W_e - (P_S + 1)/\tau_{\parallel B}, \\
dP_I/dt &= -(P_S + P_I) \cdot W_e - P_I/T_{\parallel A}.
\end{aligned} \tag{33}$$

The steady-state saturation condition ($W_e \gg 1/T_{\parallel A}$) of the transition $|1,1\rangle \Rightarrow |1,-1\rangle$ gives rise to the equalization of the populations $p(1,1) = p(1,-1)$ and to the *full nuclear spin polarization* respectively

$$P_I = -P_S = p(0,0) = 1. \tag{34}$$

It is obvious that this state is equivalent to the state with nuclear spin temperature $T_I < \hbar\omega_A/k \sim 10^{-3}$ K.

Let us estimate finally the needed microwave power for saturation. The rate of external microwave field that induces forbidden electron transitions W_S differs from the rate of allowed transitions with a flip of only one nuclear spin W by small factor that is proportional to $(B_S/B)^2$ [6], where for isotrope hyperfine interaction B_S is the field due to the dipole-dipole interaction between nuclear and electron spins of ^{31}P atom. Let us write

$$W_S \sim (\gamma_e b_{\text{mw}})^2 \cdot \tau_{\perp S}^*/2, \tag{35}$$

where $(\Delta\omega_S^2)^{1/2} \approx 2\tau_{\perp S}^{*-1}$ is the *nonhomogeneous broadened* resonance line width for the saturated electron transition, $\tau_{\perp S}^*$, is effective transverse relaxation time of electron spins, b_{mw} is the amplitude of *microwave field*.

As a result the saturation condition takes the form

$$W_S > 1/\tau_{\parallel S}, T_{\parallel A} \quad \text{or} \quad W > 1/\tau_{\parallel B}, \quad (\gamma_e b_{\text{mw}})^2 \cdot \tau_{\perp S}^* \tau_{\parallel B} > 1, \tag{36}$$

that is the same form as for allowed transition. By using expression for quality factor Q_c of microwave cavity

$$Q_c \approx \omega_S b_{\text{mw}}^2 \cdot V_r / (2\mu_0 P), \tag{37}$$

where V_r is volume of microwave resonator, P is dissipated power we will obtain the following saturation condition

$$W_e \gg 1/T_{\parallel S} \quad \text{or} \quad (\gamma_e b_{\text{mw}})^2 T_{\perp S}^* T_{\parallel S} \gg 1. \tag{38}$$

The dissipated power in cavity for $(\gamma_e b_{\text{mw}})^2 \cdot \tau_{\perp S}^* \tau_{\parallel B} = 1$ is determined by

$$P > \omega_S V_r W (\Delta\omega_S^2)^{1/2} / (2\mu_0 Q_c \gamma_e^2). \tag{39}$$

For example, taking $W \sim 1/\tau_{\parallel B} \sim 10^3 \text{ s}^{-1}$, $\omega_S \sim 100 \text{ radGHz}$, $V_r \sim 1 \text{ cm}^3$, $Q_c \sim 1000$ and $(\Delta\omega_S^2)^{1/2} \sim 10^8 \text{ s}^{-1}$ [20] as a rough estimate we obtain $P > 1 \text{ mW}$. Notice that this power is applied only during the saturation process over the time $\geq W_e^{-1} \sim 1 \text{ ms}$ in the act of qubit state initialization.

Hence, the initialization of nuclear states may be obtained by using ENDOR technique at the lattice temperature of the order of 0.1 K and by this means that *the second difficulty* of Kane's scheme can be overcome.

Notice here that there is also another possibility of ensemble NMR implementation, which does *not have the gate system*. The selectivity of nuclear resonance frequencies for individual qubit in the ensemble of Kane's chains can be achieved, rather than using the \mathbf{A} -gate voltage, with the applying of the external magnetic field gradients along axis x . For neighboring qubits separated by ~ 20 nm it is required $dB_z/dx \sim 1$ T/cm (that is feasible now), which produce a resonance frequency difference ~ 100 Hz.

There was proposed previously an all silicon NMR quantum computer where qubits are ^{29}Si nuclear spins arranged as chains in a ^{28}Si matrix [20] and with natural crystals of calcium hydroxyapatite, involving one-dimensional hydrogen chains [21], in both cases nuclear resonance frequencies are separated by a magnetic field gradient. However, in this case too large field gradient, of the order of 1 T/ μm is required.

6 The nuclear spin states decoherence due to hyperfine interaction of nuclear and electron spins

The relaxation of nonequilibrium state of the nuclear spin system represented by the product of independent (nonentangled) one-qubit states, owing to the interaction with isotropic environment, shows two processes. One is a slow establishment of equilibrium state associated with dissipation of energy. For it the diagonal elements of density matrix decay with characteristic longitudinal (spin-lattice) relaxation time T_{\parallel} . The decay of non-diagonal matrix elements called decoherence of quantum states is characterized by a decoherence time T_d or transverse (spin-spin) relaxation time T_{\perp} . The longitudinal relaxation times T_{\parallel} in the case of nuclear spin of ^{31}P atoms as qubits is defined mainly by thermal modulation of qubit resonance frequency accompanied by spin flips. It is usual that for solids $T_{\perp} \ll T_{\parallel}$.

The *internal adiabatic decoherence* mechanisms due to a random modulation of qubit resonance frequency, produced by local fluctuating magnetic fields without spin flips. These fields are determined by secular parts of interactions of nuclear spins with electron spin of the basic phosphorus atoms, with impurity paramagnetic atoms and also with nuclear spins of impurity atoms. We have named this mechanism as *internal*. It seem to be the leading one.

The modulation of nuclear spin resonance frequency $\Delta\omega(t)$, which is determined by the secular part of hyperfine interaction, may be written as

$$\Delta\omega(t) = A(t)S_z(t) - A_0 \langle S_z \rangle \approx A_0(S_z(t) - \langle S_z \rangle) - \Delta A(t) \langle S_z \rangle, \quad (40)$$

where $A(t) = A_0 + \Delta A(t)$, $\Delta A(t)$ is the modulation of hyperfine interaction constant, $A_0 = 725$ radMHz. The influence of gate voltage noise on this frequency modulation was studied in [9, 10, 23] and it is not treated here (*external* decoherence process).

Another (internal) modulation mechanism of $A(t)$ is the interaction of donor atoms with acoustic phonons. It is our belief that for very low temperature this mechanism is not essential [24].

Let us consider now the first term in (40). We shall follow the semiclassical model of *adiabatic decoherence of one-qubit state* (Appendix **A.2**). The correlation function of frequency modulation $\Delta\omega_S(t) = A_0(S_z(t) - \langle S_z \rangle)$ is determined by the fluctuations of electron spin polarization and depends on electron resonance frequency ω_S , longitudinal τ_1 (hours) and transverse τ_2 relaxation times. In adiabatic case $\omega_S = \gamma_S B > 1/\tau_2 \gg 1/\tau_1$ and we will obtain:

$$\langle \Delta_S\omega(t)\Delta\omega_S(0) \rangle = \langle \Delta\omega_S^2 \rangle \cdot \exp(-t/\tau_1), \quad (41)$$

where

$$\langle \Delta\omega_S^2 \rangle = A_0^2 \left(\langle S_z^2 \rangle - \langle S_z \rangle^2 \right) = A_0^2 (1 - \tanh^2(\gamma_S \hbar B / 2kT)) / 4. \quad (42)$$

Now, according to (74), we obtain

$$\Gamma(t) = \langle \Delta\omega_S^2 \rangle \tau_1^2 (t/\tau_1 - 1 + \exp(-t/\tau_1)). \quad (43)$$

For $\tau_1 \approx 10^4$ s and $t \sim T_d = 1$ s, $1 \ll \langle \Delta\omega_S^2 \rangle \tau_1^2 < (\tau_1/T_d)^2$ we have the non-Markovian random process (slow dampening fluctuations). In this case

$$\Gamma(t) = \langle \Delta\omega_S^2 \rangle t^2/2 \quad (44)$$

and the effective decoherence time can be estimated from $T_d \sim \langle \Delta\omega_S^2 \rangle^{-1/2}$.

The necessary value of decoherence time for the NMR quantum computer clock time $\sim 10^{-4}$ s should not exceed several seconds. Therefore, let us write the requirement for $\gamma_e \hbar B/kT \gg 1$ in the form

$$1/T_d^2 \approx A_0^2 (1 - \tanh^2(\gamma_e \hbar B/2kT))/4 \approx 2A_0^2 \exp(-\gamma_e \hbar B/kT) < 1 \text{ s}^{-2}, \quad (45)$$

from which we find that the decoherence suppression will be achieved only at *sufficiently large* $B/T > 30$ T/K. It corresponds to $B = 2$ T for lattice temperatures $T < 0.06$ K.

7 The adiabatic nuclear spin states decoherence due to interaction with nuclear spins of impurity atoms.

The paramagnetic impurity atoms having magnetic moments play also a role of environment for nuclear spins in solid state. However decoherence mechanism due to dipole-dipole interaction of their magnetic moments with nuclear spins-qubits is suppressed to a large extent at $B/T > 30$ T/K thanks to near-full electron spin polarization [24].

Another mechanism of one qubit state decoherence is dipole-dipole interaction with not fully polarized nuclear spins $I \neq 0$ of impurity diamagnetic atoms having concentration $C_{I,\text{imp}}$. Isotope ^{29}Si with $\gamma_{I,\text{imp}} = -53$ radMHz/T is one of such atoms. The random fluctuating local field, produced by nuclear spins of impurity atoms has the form

$$\Delta B_\alpha(t) = -\sum_{i,\beta}^N D_{\alpha,\beta}(\mathbf{r}_i) (I_{\beta,\text{imp}}(\mathbf{r}_i, t) - \langle I_{\beta,\text{imp}}(\mathbf{r}_i) \rangle) \quad (46)$$

where

$$D_{\alpha,\beta}(\mathbf{r}_i) = \frac{\mu_0 \gamma_I \gamma_{I,\text{imp}}}{4\pi r_i^3} \left(\delta_{\alpha\beta} - \frac{3r_{i\alpha} r_{i\beta}}{r_i^2} \right), \quad (47)$$

\mathbf{r}_i is the distance-vector to i -th impurity nuclear spin.

In this case correlation function of frequency modulation

$$\langle \Delta\omega_S(t) \Delta\omega_S(0) \rangle = \gamma_I^2 \langle B_z(t) B_z(0) \rangle = C_{I,\text{imp}} \int \sum_{\beta} D_{z,\beta}(\mathbf{r}) (I_{\beta,\text{imp}}(\mathbf{r}, t) I_{\beta,\text{imp}}(\mathbf{r}) - \langle I_{\beta,\text{imp}}(\mathbf{r}) \rangle^2) d\mathbf{r} \quad (48)$$

takes the form

$$\langle \Delta\omega_S(t) \Delta\omega_S(0) \rangle = \langle \Delta\omega^2 \rangle \exp(-t/T_{\parallel,\text{imp}}), \quad (49)$$

where $T_{\parallel,\text{imp}} \approx 10^4$ s is impurity nuclear spin longitudinal relaxation time of isotope ^{29}P at low temperature [18]. Taking $T_{\parallel,\text{imp}}$ to be much more than $T_d \sim 1$ s, for the determination of allowable impurity concentration we obtain equation

$$1/T_d^2 \approx C_{I,\text{imp}} \cdot \frac{(\mu_0 \gamma_I \gamma_{I,\text{imp}} \hbar)^2}{60\pi a^3} \cdot \left(1 - \tanh^2(|\gamma_{I,\text{imp}}| \hbar B/2kT_I) \right), \quad (50)$$

where a is minimal distance to impurity nuclear spin which for Si is of the order of $5 \cdot 10^{22} \text{cm}^{-3}$.

For $B/T > 30 \text{ T/K}$ and for spin temperature T_I at which there is near-full polarization of nuclear spins

$$|\gamma_{I,\text{imp}} \hbar B / k T_I| > 1 \quad (51)$$

or for $T_I < 0.8 \text{ mK}$, we will obtain that the allowed concentration of the isotope ^{29}Si is

$$C_{I,\text{imp}} \% < 4.5 \cdot 10^{-2} \% \quad (52)$$

This value can be increased due to the further decrease of nuclear spin temperature T_I . For comparison, natural abundance of isotope ^{29}Si in natural silicon is 4.7%. At present the realized degree of cleaning ^{28}Si is 99.98%, which does *not fully suit* for our purposes yet.

8 Adiabatic decoherence of entangled two qubit states

In the processes of input of information and logic operation performance some nonentangled initializing states of quantum register become entangled. The adiabatic process of transverse relaxation may be also the main decoherence mechanism of coherent entangled quantum states.

As a simple example let us consider here the adiabatic decoherence of the pure fully entangled two qubit triplet state EPR-type $|\psi_{\text{EPR}}\rangle = \sqrt{1/2}(|\uparrow\downarrow\rangle + |\downarrow\uparrow\rangle)$ with the zeroth projection of the total spin on z-axis, which has density matrix

$$\rho_{\text{EPR}} = |\psi_{\text{EPR}}\rangle \langle \psi_{\text{EPR}}| = \frac{1}{2} \begin{pmatrix} 0 & 0 & 0 & 0 \\ 0 & 1 & 1 & 0 \\ 0 & 1 & 1 & 0 \\ 0 & 0 & 0 & 0 \end{pmatrix}. \quad (53)$$

The action of the environment on qubit states will be described quasiclassically as correlated random modulation of the qubits resonance frequencies $\Delta\omega_{1,2}(t)$ and of indirect spin-spin interaction parameter $\Delta\omega(t) = \Delta I_I(t)/2$. The secular part of Hamiltonian for interaction with the environment is represented by

$$\begin{aligned} \mathbf{H}(t) = & -\Delta\omega_1(t)(\sigma_{1z} \otimes \mathbf{1})/2 - \Delta\omega_2(t)(\mathbf{1} \otimes \sigma_{2z})/2 + \\ & + \Delta\omega_I(t)(\sigma_{1z} \otimes \sigma_{2z})/2, \end{aligned} \quad (54)$$

where $\sigma_{1z,2z}$ are Pauli matrix.

The density matrix (53) under the action of random field in rotating frame with resonance frequency ω_0 is described by expression

$$\rho_{\text{EPR}}(t) = \mathbf{U}(t)^{-1} \rho_{\text{EPR}} \mathbf{U}(t). \quad (55)$$

In the considered case unitary matrix 4×4 $\mathbf{U}(t)$ is ($\varphi_{1,2}(t) = \int_0^t \Delta\omega_{1,2} dt$, $\varphi_I(t) = \int_0^t \Delta\omega_I dt$):

$$\begin{aligned} \mathbf{U}(t) = & (\cos(\varphi_1(t)/2)\mathbf{1} + i \sin((\varphi_1(t)/2)\sigma_{1z}) \otimes (\cos(\varphi_2(t)/2)\mathbf{1} + i \sin((\varphi_2(t)/2)\sigma_{2z}) \cdot \\ & \cdot (\cos \varphi_I(t)(\mathbf{1} \otimes \mathbf{1}) + i \sin \varphi_I(t)(\sigma_{1z} \otimes \sigma_{2z})). \end{aligned} \quad (56)$$

For perturbed density matrix we obtain

$$\rho_{\text{EPR}}(t) = \frac{1}{2} \begin{pmatrix} 0 & 0 & 0 & 0 \\ 0 & 1 & \exp(-i(\varphi_1(t) - \varphi_2(t))) & 0 \\ 0 & \exp(i(\varphi_1(t) - \varphi_2(t))) & 1 & 0 \\ 0 & 0 & 0 & 0 \end{pmatrix}. \quad (57)$$

We see that the *modulation of spin-spin interaction has no effect* on density matrix of triplet EPR-state.

Let us assume now that the random phases $\varphi_{1,2}(t)$ have mean value $\langle \varphi_{1,2}(t) \rangle = 0$ and belong to the reduced statistical ensemble, which is described by *two-dimension Gaussian distribution*:

$$w(\varphi_1(t), \varphi_2(t)) = \frac{1}{2\pi\sigma_1(t)\sigma_2(t)\sqrt{(1-\rho_{12}^2(t))}} \cdot \exp\left\{-\frac{1}{2(1-\rho_{12}^2(t))} \cdot \left(\frac{\varphi_1^2(t)}{\sigma_1^2(t)} - \frac{2\rho_{12}(t)\varphi_1(t)\varphi_2(t)}{\sigma_1(t)\sigma_2(t)} + \frac{\varphi_2^2(t)}{\sigma_2^2(t)}\right)\right\}. \quad (58)$$

Here

$$\sigma_{1,2}^2(t) = \langle \varphi_{1,2}^2(t) \rangle = 2 \int_0^t (t-\tau) f_{1,2}(\tau) d\tau$$

are the variances and

$$\rho_{12}(t) = \frac{\langle \varphi_1(t)\varphi_2(t) \rangle}{\sigma_1(t)\sigma_2(t)} = \frac{2 \int_0^t (t-\tau) f_{12}(\tau) d\tau}{\sigma_1(t)\sigma_2(t)}, \quad (59)$$

where

$$f_{1,2}(\tau) = \langle \Delta\omega_{1,2}(\tau)\Delta\omega_{1,2}(0) \rangle, \quad f_{12}(\tau) = \langle \Delta\omega_1(\tau)\Delta\omega_2(0) \rangle. \quad (60)$$

The normalized mutual correlation function $\rho_{12}(t)$ takes values in interval

$$0 \leq \rho_{12}(t) \leq 1.$$

After an averaging (57) with (58) we have

$$\langle \rho_{\text{EPR}}(t) \rangle = \frac{1}{2} \begin{pmatrix} 0 & 0 & 0 & 0 \\ 0 & 1 & \exp(-\Gamma(t)) & 0 \\ 0 & \exp(-\Gamma(t)) & 1 & 0 \\ 0 & 0 & 0 & 0 \end{pmatrix}, \quad (61)$$

where

$$\begin{aligned} \exp(-\Gamma(t)) &= \int_{-\infty}^{\infty} d\varphi_1 \int_{-\infty}^{\infty} d\varphi_2 w(\varphi_1, \varphi_2) \exp(\pm i(\varphi_1 - \varphi_2)) = \\ &= \exp\{-(\sigma_1^2(t) - 2\sigma_1(t)\sigma_2(t)\rho_{12}(t) + \sigma_2^2(t))\}. \end{aligned} \quad (62)$$

In the absence of random field correlation $\rho_{12}(t) = 0$ decrement $\Gamma(t)$ is equal to the *sum of decrements of two* one qubit states:

$$\Gamma(t) = (\sigma_1^2(t) + \sigma_2^2(t))/2 = 2\Gamma_1(t). \quad (63)$$

In case of maximum correlation $\rho_{12}(t) = 1$ and $\varphi_1(t) = \varphi_2(t)$ (the same mode acts on both qubits) *adiabatic decoherence disappears*. Analogous properties have the singlet EPR state.

We see here, that decoherence of interacted qubits states may differ essentially from one qubit decoherence. Under the action of fully correlated random fields the coherence of two mentioned entangled states is not violate and they may be considered as the basis of decoherence-free substrate for logical qubits coding. Clearly the pure nonfully entangled states $|\psi\rangle = (\sqrt{1-\alpha}|\uparrow\downarrow\rangle + \sqrt{\alpha}|\downarrow\uparrow\rangle)$ have no such properties.

Adiabatic decoherence of other two qubits fully entangled quantum Bell states $|\psi\rangle = \sqrt{1/2}(|\uparrow\uparrow\rangle \pm |\downarrow\downarrow\rangle)$ under the action of fully correlated random fields with $\rho_{12}(t) = 1$ now does not disappear. Its decrement is now equal to $\Gamma(t) = (\sigma_1(t) + \sigma_2(t))^2/2 = 2\sigma_1^2 = 4\Gamma_1(t)$, that is *four times larger* than for one qubit decoherence.

9 An antiferromagnet-based ensemble NMR quantum computer of cellular-automaton type

For implementation of ensemble silicon quantum computer, operating on cellular-automaton principle, it may be usable the previously considered ensemble of long chains of donor atoms ^{31}P disposed in silicon, but free of the **A** and **J** gates.

If exchange interaction constant (it is here positive) for localized electronic spins of ^{31}P along the chain is more than Zeeman energy $J(l) \gg \gamma_e \hbar B \tau \sim 6.5 \cdot 10^{-23} \text{ J}$, that corresponds to the distance between donors $l_x \sim 20 \text{ nm}$ [10], that is the electron critical temperature (Neel temperature) will be $T_{\text{NS}} \sim 4 \text{ K}$. and the lattice temperature is well below the critical temperature for electron ordering $T < T_{\text{NS}} \sim J(l)/k$ ($k = 1.38 \cdot 10^{-23} \text{ J/K}$ is the Boltzmann constant), than the one-dimensional *antiferromagnetically ordered ground state* of electronic spins can be produced.

Due to hyperfine interaction nuclear spins will be oriented according to the electronic spin direction in the resultant field and can form array with the alternating orientation of nuclear spins. At magnetic fields $B < A/\gamma_I \hbar \sim 3.5 \text{ T}$ and at spin temperatures $T \sim 10^{-3} \text{ K}$ the nuclear spins ^{31}P will form a periodic ground state array of ABAB... type: $\uparrow \downarrow \uparrow \downarrow \dots$, where \uparrow marks the ground state of nuclear spin in an A-site and \downarrow is the ground state of nuclear spin in a B-site with almost 100% opposite orientation ($\omega_{\text{A,B}}/kT \geq 1$). That is the distinct nuclear spins will be *in initialized ground state*.

Notice that the using of dynamic methods makes possible the high orientation of nuclear spins also at larger lattice temperatures, this state will be *the long-lived nonequilibrium* nuclear spin state.

The nuclear resonant frequencies $\omega_{\text{A,B}}$ of neighboring nuclear spins are different for each of the magnetic one-dimensional subarray A and B in the chain as they depend on the states of neighboring spins. We will take it here in the simple form [14, 25, 26]:

$$\omega_{\text{A,B}} \equiv \omega(m_{<} + m_{>}) \approx |\gamma_I \hbar B \pm A/2 - I_n \cdot (m_{<} + m_{>})| / \hbar, \quad (64)$$

where I_n is constant of two neighboring nuclear indirect spin-spin interaction, $m_{<} = \pm 1/2$ and $m_{>} = \pm 1/2$ are the magnetic quantum numbers for the left and right nuclear spins. The nonsecular part of nuclear-nuclear interaction is neglected here taking into account that $\gamma_I \hbar B, A/2 \gg I_n$. The difference between nuclear resonant frequencies for the distinct neighboring spin orientations is $\Delta\omega_I/2\pi \sim I_n/2\pi\hbar \sim 0.5 \text{ MHz}$, whereas the resonant nuclear frequencies are $\omega_{\text{A,B}}/2\pi \sim A/4\pi\hbar \sim 120 \text{ MHz}$.

For the organization of logic operations let us use the addressing to spin states, similar to the scheme put forward in [27]. Each nuclear spin in A-site of this scheme has *two internal* eigenstates – ground $|\uparrow\rangle$ and excited $|\downarrow\rangle$ and in B-site – $|\downarrow\rangle$ and $|\uparrow\rangle$ accordingly.

We take into account that the life time of excited states (the longitudinal nuclear spin relaxation time $T_{||}$) at low temperatures is very long. Each *logic qubit* of quantum information in this state will be encoded here, similar to [27], by the *states of four physical spin-qubits*: the logical qubit basis state "0" will be encoded by unit $|\downarrow\uparrow\uparrow\downarrow\rangle$, while the state "1" will be encoded by $|\uparrow\downarrow\downarrow\uparrow\rangle$. It is important here that the resonance frequencies of nuclear spins depend on neighboring spin states. Both logical states have two excited spin states and *zero projection* of total nuclear spin.

Notice that a random inversion of only one spin will result in degradation of the qubit state. But to form the rough error, for example, of "0" \Rightarrow "1" type in the coding of stored quantum information it is essential to invert *four* spins *simultaneously*. Therefore, it may be concluded that the considered way of qubit coding ensures *a better fault-tolerance* with respect to this type of errors.

The input and output of the information in the array of ground states spins could be performed at the ends of the array, where the nuclear spins (say in A-site at the left end) have only one neighboring spin and resonant frequency $\omega_{\text{A}}(-1/2)$ ($m_{<} + m_{>} = -1/2$). The corresponding selective resonance $\pi_{\text{A},-1/2}$ -pulse inverts only one nuclear spin (in A-site) at the end of array and doesn't influence other ones. Then the new selective $\pi_{\text{B},0}$ -pulse will invert next nuclear spin (in B-site), which has the opposite orientation of ground and excited neighbor nuclear spin ($m_{<} + m_{>} = 0$ in A-site) and consequently the new resonant frequency, distinguished from the frequency of spins with the neighbor nuclear spin in the same ground states ($m_{<} + m_{>} = 1$) (See Table).

Table. The π -pulses for spins in A- and B-sites

Neighbor spin states A-site	A \downarrow	\downarrow A \downarrow	\downarrow A \uparrow	\uparrow A \downarrow	\uparrow A \uparrow
Resonance frequency	$\nu_A(-1/2)$	$\nu_A(-1)$	$\nu_A(0)$	$\nu_A(0)$	$\nu_A(1)$
π -pulses	$\pi_{A,-1/2}$	$\pi_{A,-1}$	$\pi_{A,0}$	$\pi_{A,0}$	$\pi_{A,1}$
Neighbor spin states B-site	B \downarrow	\uparrow B \uparrow	\uparrow B \downarrow	\downarrow B \uparrow	\downarrow B \downarrow
Resonance frequency	$\nu_B(1/2)$	$\nu_B(1)$	$\nu_B(0)$	$\nu_B(0)$	$\nu_B(-1)$
π -pulses	$\pi_{B,1/2}$	$\pi_{B,1}$	$\pi_{B,0}$	$\pi_{B,0}$	$\pi_{B,-1}$

Thus the logical qubit state "0", that is $|\underline{\downarrow}\underline{\uparrow}\underline{\uparrow}\underline{\downarrow}\rangle$, is formed in the following way (the pulses act on underlined spins from the left):

$$\begin{array}{c} \underline{\uparrow}\underline{\downarrow}\underline{\uparrow}\underline{\downarrow} \dots \pi_{A,-1/2} \\ \underline{A} \underline{B} \underline{A} \underline{B} \end{array} \Rightarrow \begin{array}{c} \underline{\downarrow}\underline{\downarrow}\underline{\uparrow}\underline{\downarrow}\underline{\uparrow} \dots \pi_{B,0} \\ \underline{A} \underline{B} \underline{A} \underline{B} \end{array} \Rightarrow \begin{array}{c} \underline{\underline{\downarrow}}\underline{\underline{\uparrow}}\underline{\underline{\uparrow}}\underline{\underline{\downarrow}} \dots \\ \underline{A} \underline{B} \underline{A} \underline{B} \end{array}$$

As the *ports* (noted in Fig. 5 by cross 'x') for input and output of the information in the array of ground states spin-qubits can be also dopant nuclei D at the certain place of the array with distinct resonant frequency, defects or local gates that modify the resonant frequency of the nearest nuclear spin in the array.

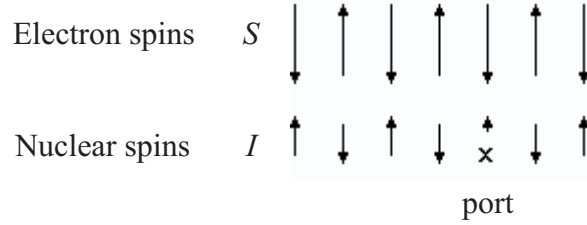


Fig. 5. Scheme of electron and nuclear spins ordering.

Starting from the perfectly initialized states inputting the information can be performed by setting the dopant D-spin to a desired state by means of RF-pulse at its resonant frequency. The nuclear spin state of spin nearest to the dopant spin is created by SWAP operation. After the required information is loaded, D-spin is reset to the ground state. Upon completion of computation, the state of any spin can be measured by moving it to the A-site nearest to D, then swapping $A \Rightarrow D$ and finally measuring the state of D-spin.

For the implementation of quantum operations on logic qubits we will also introduce one auxiliary control unit (CU), which is represented here by *six* physical spin states in the pattern $\underline{\uparrow}\underline{\downarrow}\underline{\downarrow}\underline{\uparrow}\underline{\uparrow}\underline{\downarrow}$. The CU exists only in one place along the array and is separated from logical qubits by odd number of spacer spins. The applying of corresponding SWAP sequence of pulses CU leads to putting the interaction of CU with one and two logical qubits and performing on them one- and two-qubit quantum operations (for more details, see [14, 25, 26]).

In the case of a large enough ensemble of in parallel acting chains the states may be measured by NMR methods. For the increasing of logic qubit number in single 'molecule' to $\geq 10^3$, that falls on one port, two- and three-dimensional structures with antiferromagnetic chess-type ordering of electron spins may be used. The corresponding ordering will also be for nuclear spins (Fig. 6).

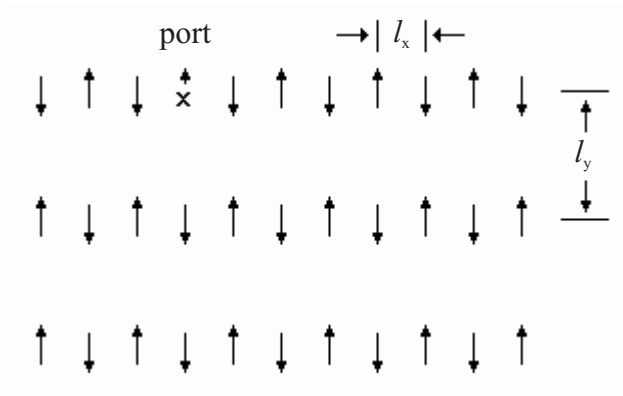


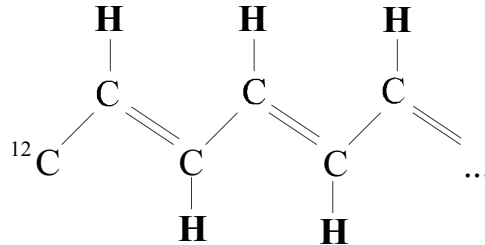
Fig. 6. Scheme of two dimensional chess-type ordering of initialized nuclear spins.

If, for example, the number of spins-qubits, falls on one port in linear chain is, say, $L \sim 30$, so in two-dimension case their number will be $L = 900$. Ensemble that is composed of $N \sim 10^5$ in parallel acting such plane ‘artificial molecules’ permit to provide input and output of information through the standard NMR techniques. The using of more sensitive ENDOR techniques has particular meaning when it may be combined with the techniques of dynamic polarization (solid state effect).

Structures with two and three-dimensional antiferromagnetic order may be found perhaps among the *natural rare earth* or *transition element* dielectric compounds.

There are the rare earth compounds of *thulium* stable isotope ^{169}Tm , that has nuclear spin $I = 1/2$, $g_N = 0.458$ and makes up 100% of abundance, with stable spinless isotopes of other elements Tm. They can be possible: Tm_2O_3 , TmSi_2 , TmGe_2 , TmSe . The natural elements O, Si, Ge and Se have, accordingly, nuclear spin containing isotopes (in brackets the isotope abundance is shown) ^{17}O $I = 5/2$ (0.04%), ^{29}Si $I = 1/2$ (4.7%), ^{73}Ge $I = 9/2$ (7.76%), ^{77}Se $I = 1/2$ (7.78%). The choosing the needed compounds requires further detailed theoretical and experimental investigations.

It may be also considered, as variant for ensemble NMR quantum computer, organic dielectric crystals, containing quasi-one-dimensional chains, such as antiferromagnetically ordered chains of polyacetylene with only proton nuclei, for qubits:



The advantages of ensemble quantum cellular automaton in comparison with the above considered ensemble variant with strip gates are as follows:

- a) The system of the control gates is absent, what essentially simplifies the production of computer structure and eliminates one of the important sources of decoherence.
- b) The coding of logic qubits into four physical qubits gives a higher degree of fault-tolerance in logic operations.

It follows that the going to ensemble quantum cellular automaton permits to overcome *the third and fourth* difficulties of Kane’s scheme.

The chief disadvantage of cellular automaton scheme is the relative complexity of logic operation performance.

Conclusion

1. The line of the large-scale ensemble NMR quantum computer development has certain advantage over Kane's scheme. It consists in the possibility of employment of the standard NMR technique for the measurement of quantum states at output of computer, like in the liquid prototype.
2. For the initialization of nuclear spin states at temperature $T \sim 0.1$ K methods of dynamic polarization may be proposed.
3. Analysis of proposed planar structure of ensemble silicon computer shows the possibility of realization of large-scale NMR quantum computer for ensemble component number $N \sim 10^5$.
4. The main reasons for the internal decoherence of one qubit states are the modulation of resonance qubit frequency due to hyperfine interaction with fluctuating electron spin and due to interaction with randomly distributed impurity diamagnetic atoms containing nuclear spins.
5. Analysis of different feasible ways for obtaining decoherence times large enough shows that the values, needed to perform the required for large-scaled computations number of quantum logic operations $\sim 10^5$, can be achieved.
6. The implementation of cellular automaton principle permits to abandon the realization regular nanostructure in the form of gate chains.

Appendix

A1. Signal NMR for discrete ensemble of nuclear spins

Let us consider here the sample that involves $N = nL \cdot pN_0$ nuclear spin-qubits arranged in the plane $z = 0$ of the silicon plate at regular intervals along the strips (Fig. 4). The spins in chains under strip at resonance in each block are oriented along x axis (solenoid axis) and separated at intervals of L . The read out NMR signal is

$$|V_{\max}| = Q\omega_A \frac{K}{X} \int_{-X/2}^{X/2} \left| \int_A B_{x\max}(x, y, z) dy dz \right| dx, \quad (65)$$

where $X = nL \gg L$ is roughly the length of solenoid and

$$B_{x\max}(x, y, z) = \frac{\mu_0 \gamma \hbar}{16\pi} \sum_{n_i=-n/2}^{n/2} \sum_{p_i=-pN_0/2}^{pN_0/2} \frac{-2(x - Ln_i)^2 + (y - l_y p_i)^2 + z^2}{[(x - Ln_i)^2 + (y - l_y p_i)^2 + z^2]^{5/2}} \quad (66)$$

is the peak magnetic field produced by resonant spins in solenoid. For simplicity it is suggested that $n, p, N_0, L \gg 1$ are the even numbers. We assume that the area of coil turns is $A = D \cdot \delta$ ($D = l_y \cdot pN_0$, $\delta \ll D$).

For summation over n_i and p_i we have used the *Poisson summation formula*, namely,

$$\sum_{p_i=-pN_0/2}^{pN_0/2} f(l_y p_i) = \frac{pN_0}{D} \sum_{\nu=-\infty}^{\infty} \int_{-D/2}^{D/2} f(\xi) \exp(i\nu 2\pi \xi / l_y) d\xi, \quad (67)$$

by omitting the oscillated terms with $\nu \neq 0$:

$$|V_{\max}| = \mu_0 Q K \omega_A \frac{\gamma \hbar}{8\pi} \frac{1}{X} \int_{-X/2}^{X/2} dx \frac{n}{X} \int_{-X/2}^{X/2} d\eta \cdot \int_0^{\delta/2} dz \left| \frac{pN_0}{D} \int_{-D/2}^{D/2} \int_{-D/2}^{D/2} \frac{-2(x - \eta)^2 + (y - \xi)^2 + z^2}{[(x - \eta)^2 + (y - \xi)^2 + z^2]^{5/2}} dy d\xi \right| \quad (68)$$

Taking into account $D^2 \gg z^2$, upon integrating (67) over y, ξ , we obtain

$$|V_{\max}| = \mu_0 Q K \omega_A \frac{\gamma_1 \hbar p N_0}{8\pi} \frac{1}{D} \frac{1}{X} \int_{-X/2}^{X/2} dx \frac{n}{X} \int_{-X/2}^{X/2} d\eta \cdot \int_0^{\delta/2} dz \left(\frac{2[(x-\eta)^2 - z^2]D^2}{[(x-\eta)^2 + z^2]^2 [D^2 + (x-\eta)^2]^{1/2}} + \frac{2z^2}{[(x-\eta)^2 + z^2]^{3/2}} \right). \quad (69)$$

By integrating now over z and preserving only the major logarithmically increasing for $2|x-\eta|/\delta \Rightarrow 0$ term, we obtain

$$\begin{aligned} |V_{\max}| &\approx \mu_0 Q K A \omega_A \frac{\gamma_1 \hbar np N_0}{4\pi} \frac{1}{AD} \frac{1}{X} \int_{-X/2}^{X/2} dx \frac{1}{X} \int_{-X/2}^{X/2} d\eta \log \frac{\delta}{|x-\eta|} = \\ &= (\mu_0/4) Q K A \omega_A \frac{N}{V_s} \gamma_1 \hbar \cdot \frac{X}{\pi D} \log \frac{X}{\delta \sqrt{e}}, \end{aligned} \quad (70)$$

where $V_s = AX$, $N = npN_0$, $e = 2.718\dots$

We see that expression (A.7) is distinguished from (4) by non-essential factor $\frac{X}{\pi D} \log \frac{X}{\delta \sqrt{e}}$, that is of the order of several ones.

A2. Semiclassical model of adiabatic decoherence of one-qubit state

We will consider a long-lived non-equilibrium qubit state when diagonal elements of density matrix may be treated as a constant.

The random modulation of resonance frequency $\Delta\omega(t)$ that causes the dephasing of a qubit state is determined by the random phase shifts

$$\varphi(t) = \int_0^t \Delta\omega(t) dt. \quad (71)$$

The one-qubit density matrix of pure state in rotating frame with non perturbed resonance circular frequency will be

$$\rho(t) = 1/2 \begin{bmatrix} 1 + P_z & P_- \exp(i\varphi(t)) \\ P_+ \exp(-i\varphi(t)) & 1 - P_z \end{bmatrix}, \quad (72)$$

where $P_{\pm} = P_x \pm iP_y$, P_x, P_y, P_z are Bloch vector components of length $P = \sqrt{P_x^2 + P_y^2 + P_z^2} = 1$.

By treating the resonance frequency modulation as Gaussian random process after averaging (72) over phase distribution with $\langle \varphi(t) \rangle = 0$ we obtain

$$\langle \rho(t) \rangle = 1/2 \begin{bmatrix} 1 + P_z & P_- \exp(-\Gamma(t)) \\ P_+ \exp(-\Gamma(t)) & 1 - P_z \end{bmatrix}, \quad (73)$$

where

$$\Gamma(t) = 1/2 \cdot \left\langle \left(\int_0^t \Delta\omega(t) dt \right)^2 \right\rangle = \int_0^t (t-\tau) \langle \Delta\omega(\tau) \Delta\omega(0) \rangle d\tau, \quad (74)$$

$f(t) = \langle \Delta\omega(t) \Delta\omega(0) \rangle$ is the frequency correlation function of a random process, which is characterized by variance $\langle \Delta\omega(0)^2 \rangle$ and correlation time τ_C such that for $t > \tau_C$ $\langle \Delta\omega(t) \Delta\omega(0) \rangle \Rightarrow 0$. For $\Gamma(t) > 0$ the averaged density matrix presents a mixed quantum state with two non-zero eigen states

$$1/2 \cdot \left(1 \pm \sqrt{1 - (P_x^2 + P_y^2)(1 - \exp(-2\Gamma(t)))} \right) \quad (75)$$

and the populations of states $p_{\pm} = 1/2(1 \pm P_z(0))$ at $\Gamma(t) \Rightarrow \infty$.

Thus, the adiabatic decoherence problem is reduced to the determination of the function $\Gamma(t)$ or the correlation function of random frequency modulation.

In the case of an ensemble quantum register there is a need to average the one-qubit density matrix and correlation function over ensemble of independent equivalent spins-qubits.

References

- [1] N. A. Gershenfeld, I. L. Chuang. Bulk Spin-Resonance Quantum Computation, *Science*, 1997, vol. 275, pp. 350–356.
- [2] I. L. Chuang, N. Gershenfeld, M. G. Kubinec, D. W. Leung. Bulk Quantum Computation with Nuclear Magnetic Resonance: Theory and Experiment, *Proc. Roy. Soc. London*, 1998, vol. A454, no. 1969, pp. 447–467.
- [3] D. G. Cory, M. D. Price, T. F. Havel. Nuclear Magnetic Resonance Spectroscopy: An Experimentally Accessible Paradigm for Quantum Computing, *Physica D*, 1997, vol. 120, no. 1–2, pp. 82–101.
- [4] D. G. Cory, A. F. Fahmy, T. F. Havel. Ensemble Quantum Computing by NMR Spectroscopy, *Proc. Nat. Acad. Sci. USA*, 1997, vol. 94, no. 5, pp. 1634–1639.
- [5] E. Knill, I. Chuang, R. Laflamme. Effective Pure States for Bulk Quantum Computation, *Phys. Rev.*, 1998, vol. A57, no. 5, pp. 3348–3363.
- [6] A. Abragam. *The Principles of Nuclear Magnetism*. Oxford, Clarendon Press, 1961.
- [7] J. A. Jones. NMR Quantum Computation: a Critical Evaluation, *Fortschr. Phys.*, 2000, vol. 48, no 9–11, pp. 909–924.
- [8] D. P. DiVincenzo. The Physical Implementation of Quantum Computation, *Fortschr. Phys.*, 2000, vol. 48, no 9–11, pp. 771–783.
- [9] B. E. Kane. A Silicon-Based Nuclear Spin Quantum Computer, *Nature* (London), 1998, vol. 393, pp. 133–137.
- [10] B. E. Kane. Silicon-based Quantum Computation, *Fortschr. Phys.*, 2000, vol. 48, no 9–11, pp. 1023–1041.
- [11] J. L. O’Brien, S. R. Schofield, M. Y. Simmons, R. G. Clark, A. S. Dzurak, N. J. Curson, B. E. Kane, N. S. McAlpine, M. E. Hawley, G. W. Brown. Towards the Fabrication of Phosphorus Qubits for a Silicon Quantum Computer, *Phys. Rev.*, 2001, vol. B64, 161401 (R), 5p.
- [12] T. M. Buehler, R. P. McKinnon, N. T. Lumpkin, R. Brenner, D. J. Really, L. D. Macks, A. R. Hamilton, A. S. Dzurak, R. G. Clark. Self-Aligned Fabrication Process for Quantum Computer Devices, E-print LANL: arXiv:quant-ph/0208374, 2002.
- [13] K. A. Valiev, A. A. Kokin. Solid-State NMR Quantum Computer with Individual Access to Qubits and Some Their Ensemble Developments, E-print LANL: arXiv:quant-ph/9909008, 1999.
- [14] K. A. Valiev, A. A. Kokin. *Quantum computers: reliance and reality*. Second edition, Moscow-Izhevsk: R&C Dynamics, 2002 (in Russian), 320 p.
- [15] G. Ludwig, and H. Woodbury. *Electron Spin Resonance in Semiconductors*, New York: Academic Press, 1962.
- [16] K. A. Valiev. Magnetic Resonance on Nuclei of Paramagnetic Atoms, *Zh. Eksp. Teor. Fiz.*, 1957, vol. 33, no. 4(10), pp. 1045–1047 (in Russian).
- [17] A. A. Kokin, K. A. Valiev. Problems in Realization of Large-Scale Ensemble Silicon-based NMR Quantum Computers, *Quantum Computers & Computing*, Moscow-Izhevsk: R&C Dynamics, 2002, vol. 3, no.1, pp. 25–45, E-print LANL: arXiv:quant-ph/0201083.
- [18] G. Feher, E. A. Gere. Electron Spin Resonance Experiments on Donors in Silicon. II. Electron Spin Relaxation Effects. *Phys. Rev.*, 1959, vol. 114, no. 5, pp. 1245–1256.

- [19] A. Abragam, M. Goldman. Nuclear Magnetism: Order & Disorder. Oxford: Claren.Press, 1982.
- [20] M. Chiba, A. Hira. Electron Spin Echo Behavior of Phosphorus Doped Silicon. *Jour. Phys. Soc. Jap.*, 1972, vol. 33, no. 3, pp. 730–738.
- [21] T. D. Ladd, J. R. Goldman, F. Yamaguchi, Y. Yamamoto, E. Abe, K. M. Itoh. An all Silicon Quantum Computer, E-print LANL: arXiv:quant-ph/0109039.
- [22] E. B. Fel'dman, S. Lacelle. Perspectives on a Solid State NMR Quantum Comhuter, E-print LANL: arXiv:quant-ph/0108106.
- [23] C. J. Welled. L. C. L. Hollenberg. Stochastic Noise as a Source of Decoherence in a Solid State Quantum Computer, E-print LANL: arXiv:quant-ph/0104055, 2001.
- [24] A. A. Kokin. Decoherence of Quantum States and its Suppression in Ensemble Large-Scale Solid State NMR Quantum Computers, E-print LANL: arXiv:quant-ph/0211096, 2002; *Proc. SPIE*, 2003, N.5128.
- [25] A. A. Kokin. An Antiferromagnet-Based NMP Quantum Computer, *The Phys. Metals and Metallogr.*, 2001, vol. 92, Suppl.1, pp. S150–S156.
- [26] A. A. Kokin. A Model for NMR Quantum Cellular Automata Using Antiferromagnetic structure. *Quantum Computers & Computing*, Moscow-Izhevsk: R&C Dynamics, 2001, vol. 2, no. 1, pp. 54–67; E-print LANL: arXiv:quant-ph/0002034, 2000.
- [27] S. C. Benjamin. Schemes for Parallel Quantum Computation Without Local Control of Qubits. *Phys. Rev.*, 2000, vol. A61, pp.020301(R).